

Polymer Coated MWCNT/Terpolymer Composites: Spectral, Thermal and Electrical Properties

Demet Coşkun*, Mehmet Fatih Coşkun and Mehmet Coşkun
Department of Chemistry, Science Faculty, Firat University, Elazığ, Turkey.
dcoskun@firat.edu.tr*

(Received on 28th October 2013, accepted in revised form 26th May 2014)

Summary: The terpolymer-1 was prepared from radicalic polymerization of (*E*)-4-[3-(benzofuran-2-yl)-3-oxoprop-1-enyl] phenyl acrylate (BPCA), 2-hydroxyethyl methacrylate (HEMA) and N-isopropylacrylamide (NIPA). The terpolymer-2 was prepared using 2-Acrylamidoglycolic acid mono hydrate (AMGA) instead of HEMA. The oxidized multi-walled carbon nanotube (MWNT-COOH) and thionylchloride (SOCl₂) was used in preparing of carbonyl chloride-functionalized carbon nanotube (MWNT-COCl). MWNT-COCl was coated separately by terpolymer-1 and terpolymer-2, heating at 120 °C for 6 h. Spectral and thermal properties, the photo-crosslinking behaviors and dielectrical and electrical properties of the terpolymers and the composites were investigated. The composite-1 exhibits a double emission wavelength at 325 nm and at 680 nm for an excitation wavelength of 530 nm. In the photo-crosslinking studies of terpolymer 1, immediately after each irradiation time intervals, the absorbance change at 345 nm was monitored. Dielectric constant is not change noticeably with temperature for nonpolar polymers whereas dielectric constant increases with temperature for strong polar polymers.

Keywords: Multi-walled carbon nanotube; Polymer composite; Spectral properties; Thermal, Dielectrical behaviors

Introduction

The properties and applications of carbon nanotubes (CNT) and related materials have been very interesting research fields in recent years [1]. CNTs have received much attention for their much potential application, such as photocatalyst [2], electrochemical [3], nanowires [4], nanoelectronic [5], photovoltaic devices [6], gas sensors [7], semiconductor [8] and nanocomposite materials [9-11].

The functionalization of defect sites at the end or side walls of the nanotubes by oxidation is a well-known functionalization technique. The oxidatively introduced carboxyl groups represent useful sites for further modifications. By this way, the nanotubes can be provided with a wide range of functional moieties. For oxidation to carboxyl group, multi-walled carbon nanotube (MWNT) is treated with H₂SO₄/HNO₃ mixture [12, 13], as an oxidizing agent. Then the carboxyl group is converted to acyl chloride using SOCl₂, which is a more active group than carboxyl group.

The combination of CNTs with polymers may offer attractive possibility to enhance the thermal, electrical, mechanical and spectrophotometric properties of polymer composites [14]. Ajayan *et al.* [15] reported the first polymer/CNT composites. The dispersion of CNTs in polymer matrices is a critical issue in preparation of CNT/polymer composites. Currently there are several

methods used to prepare CNT/polymer composites. One of them is solution mixing. In this approach, a dispersion of CNTs in suitable solvent and polymers are mixed in solution under ultrasonic irradiation, and the CNT/polymer composite is formed by precipitation of composite and by evaporation of solvent [16]. The number of research article, review article and patents written on polymer/CNT composites is increasing every year [1, 10, 17-19].

In this paper, we reported the preparation of composites of two terpolymers and multi-walled carbon nanotube (MWNT), and electrical, dielectrical, thermal and spectroscopic properties of the composites.

Experimental

Materials

MWCNT is purchased from Grafen Kim. San. Şti, and it is average diameter and average length 9.5 nm and 1.5 µm, respectively. Triethylamine, acryloyl chloride, acetylbenzofurane, 4-hydroxybenzaldehyde, SOCl₂, H₂SO₄, HNO₃, 2-hydroxyethyl methacrylate, 2-acrylamidoglycolic acid mono hydrate, N-isopropylacrylamide and 1,4-dioxane were purchased from Aldrich-Sigma and were used without any purification.

*To whom all correspondence should be addressed.

Characterization Technique

Infrared spectra were recorded on a Perkin-Elmer Spectrum One FTIR spectrometer. ^1H -NMR spectra were obtained on a 400 MHz Bruker AVIII 400 machine, using dimethyl sulfoxide (DMSO) as the solvent, and tetramethylsilane as an internal standard. Calorimetric measurements were carried out on a Shimadzu DSC-50 thermal analyzer under N_2 flow using a heating rate of $20\text{ }^\circ\text{C}/\text{min}$. Thermal stability studies were carried out on a Shimadzu TGA-50 thermobalance under N_2 flow using a heating rate of $10\text{ }^\circ\text{C}/\text{min}$.

The capacitance measurements were carried out at room temperature with a QuadTech 7600 precision LRC meter impedance analyzer over the frequency range 50 Hz-10 kHz. The polymer and the composites were ground with an agate mortar and pestle, and the final fine powders were pressed at four tons of pressure into disc-shaped samples with a thickness ranging from 0.42-0.73 mm and a diameter of 12 mm. The entire surface of the discs was coated with a silver paste, which acts as a good contact for capacitance measurements.

Synthesis of (E)-1-(benzofuran-2-yl)-3-(4-hydroxyphenyl)prop-2-en-1-one (BPC)

BPC was prepared according to the method given in literature [20], starting by 2-acetylbenzofurane and 4-hydroxybenzaldehyde.

(E)-4-[3-(benzofuran-2-yl)-3-oxoprop-1-enyl]phenyl acrylate (BPCA)

In a 50 mL three-necked flask, BFC (0.545 g, 2.06 mmol) and triethylamine (0.3 mL, 2.17 mmol) were dissolved in 10 mL THF and cooled to $0\text{ }^\circ\text{C}$. Acryloyl chloride (0.18 mL, 2.17 mmol) in 3 mL THF was then added dropwise with stirring, keeping the temperature in the range $0\text{ }^\circ\text{C}$ to $+5\text{ }^\circ\text{C}$. After complete addition of the acryloyl chloride, temperature of the reaction mixture was allowed to rise slowly to room temperature and the content was stirred for 24 h. The mixture was added to cold water and precipitate was filtered off. The product was recrystallized from methanol. Yield : 94%; m.p. $138\text{--}139\text{ }^\circ\text{C}$.

Preparation of carbonyl chloride-functionalized carbon nanotube (MWNT-COCl)

Multi-walled carbon nanotube (MWNT) was first oxidized according to the experimental procedures adapted from the literature [12, 13].

Briefly, 1.2 g MWNT, 10 mL conc. HNO_3 and 30 mL conc. H_2SO_4 were added to a 250 mL three-necked flask and was sonicated for 9 h at $80\text{ }^\circ\text{C}$. The resultant mixture was then slowly poured into 200 mL water. The diluted mixture was neutralized with 40 g NaOH in 250 mL water, filtered and washed with deionized water. The oxidized MWNT (MWNT-COOH) was filtered off, and after the solid was dried in air for a few hours, it was dried under vacuum at $60\text{ }^\circ\text{C}$ for 24 h.

Dried MWNT-COOH (0.86) was suspended in 50 mL SOCl_2 and refluxed for 24 h. The solid filtered off and washed with anhydrous CHCl_3 and dried under vacuum at room temperature.

Preparation of Terpolymer-1

A mixture of the BPCA (0.318 g, 1 mmol), N-isopropylacrylamide (NIPA) (0.396 g, 3.5 mmol), 2-hydroxyethyl methacrylate (HEMA) (0.072 g, 0.5 mmol), AIBN (0.0079 g) and anhydrous 1,4-dioxane (2 mL) were added to the polymerization tube and sealed under argon. The reaction content was heated at $60\text{ }^\circ\text{C}$ for 30 h. Then, the mixture was diluted with 2 mL 1,4-dioxane and precipitated (twice) into diethyl ether. The terpolymer-1 was dried under vacuum at $50\text{ }^\circ\text{C}$ (0.36 g, 45%).

Preparation of terpolymer-2

A mixture of the BPCA (0.30 g, 0.943 mmol), N-isopropylacrylamide (NIPA) (0.50 g, 4.4 mmol), 2-acrylamidoglycolic acid mono hydrate (AMGA, 0.154 g, 0.943 mmol), AIBN (0.0095 g) and anhydrous 1,4-dioxane (2 mL) were added to the polymerization tube and sealed under argon. The reaction content was heated at $65\text{ }^\circ\text{C}$ for 24 h. Then, the mixture was diluted with 2 mL 1,4-dioxane and precipitated (twice) into diethyl ether. The terpolymer-2 was dried under vacuum at $50\text{ }^\circ\text{C}$ (0.267 g, 28%).

Preparation of CNTs coated with terpolymers

Terpolymer-1 (0.1 g) was dissolved in 25 mL 1,4-dioxane, and added to MWNT-COCl (0.2 g) and was sonicated for 15 min. The solvent was removed by rotary evaporator. The CNT coated with terpolymer-1 (MWNT-Ter-1) was dried at $120\text{ }^\circ\text{C}$ for 6 h.

Terpolymer-2 (0.06 g) was dissolved in 25 mL 1,4-dioxane, and added to MWNT-COCl (0.12 g) and was sonicated for 15 min. The solvent was removed by rotary evaporator. The CNT coated with

terpolymer-2 (MWNT-Ter-2) was dried at 120 °C for 60 h.

Preparation of CNT/the polymer nanocomposites

The composites were prepared according to the method adapted from the literature [16]. Briefly, 0.245 g of the terpolymer-1 was dissolved in 5 mL 1,4-dioxane, and was dispersed in this solution 0.005 g of the CNT coated with terpolymer-1 (MWNT-Ter-1) by using an ultrasonic bath. The mixture was dropwise added into diethyl ether to precipitate the composite-1 (with content 1.2% MWNT), filtered, dried under vacuum at 50 °C for 24 h. Composite-2 (with content 1.2% MWNT) was prepared similarly from the terpolymer-2 and the CNT coated with terpolymer-2 (MWNT-Ter-2). The powder composites were formed in the form of pellet by applying 10 ton.

Results and Discussion

Spectral Characterization

The FT-IR spectra of MWNTs and terpolymers were presented in Fig. 1. The bands at 3430 cm⁻¹ (OH stretch vibration), 1755 cm⁻¹ (C=O stretch vibration for ester groups in chalcone units),

1725 cm⁻¹ (C=O stretch vibration for ester in HEMA units), 1655 cm⁻¹ (C=O stretch vibration for amid and ketone groups in NIPA and chalcone units), 1612 cm⁻¹ (C=C stretch vibration for in chalcone units) are attributed to the presence of the monomeric units on the terpolymer-1. The bands at 3340 cm⁻¹ (OH stretch vibration), 1755 cm⁻¹ (C=O stretch vibration for ester groups in chalcone units), 1730 cm⁻¹ (C=O stretch vibration for acid group in AMGA units), 1655 cm⁻¹ (C=O stretch vibration for amid groups in NIPA and AMGA units, and ketone groups in chalcone units), 1612 cm⁻¹ (C=C stretch vibration for in chalcone units) are attributed to the presence of the monomeric units on the terpolymer-2. In the both spectra, the isopropyl group shows two bands at 1387 and 1367 cm⁻¹ assigned to the C-H bending vibration. In the FT-IR spectra of MWNT-COOH, the bands at 3434 cm⁻¹ (O-H stretching vibration), 1711 cm⁻¹ (C=O stretching vibration) and 1630 cm⁻¹ (C=C on the MWCNT) indicate surface modification of the MWCNT. The bands at 1720 cm⁻¹ (C=O) and 1630 cm⁻¹ (C=O and C=C) and 1000-1200 cm⁻¹ (C-O) in the spectra of MWNT-Ter-1 and MWNT-Ter-2 (no spectrum) show the functional groups on the surface of the terpolymers. The FT-IR spectrum of composite-2 shows the bands at 1725 cm⁻¹ (C=O), 1632 cm⁻¹ (C=O in the amid group and C=C on the CNT) and 1000-1200 cm⁻¹ (C-O).

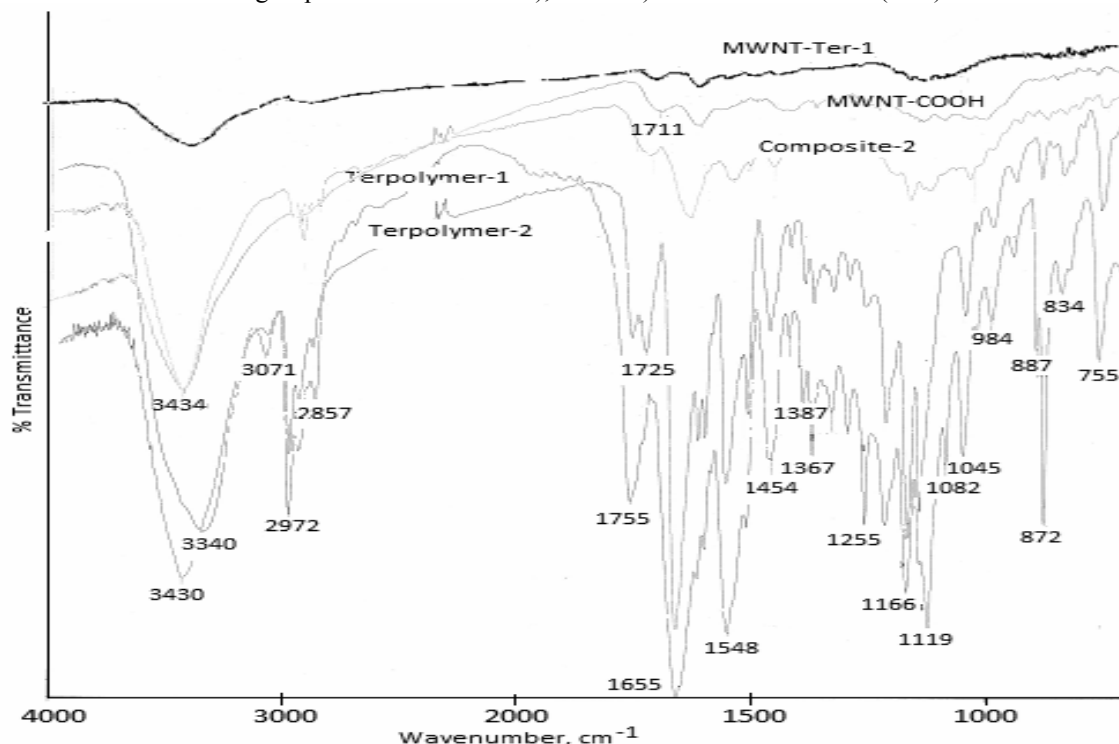


Fig. 1: The FT-IR spectra of MWNT-Ter-1, MWNT-COOH, composite-2, terpolymer-1 and terpolymer-2.

All the ^1H -NMR spectra taken from DMSO solution are shown in Fig. 2. In the spectrum of terpolymer-1, signals at 8.3 ppm ($-\text{CONH}-$), at 7.3-8.0 ppm (aromatic and olefinic protons in chalcone units), at 4.8-4.2 ppm (broad peak, $-\text{OH}$), 3.7-4.0 ppm ($-\text{NCH}-$, $-\text{COOCH}_2\text{CH}_2\text{O}-$) and 0.8-2.3 ppm (CH_3 , CH_2 and CH) are confirm the structure. The ^1H -NMR spectrum of terpolymer-2 contains signals at 12.9 ppm ($-\text{COOH}$), 8.3 ppm (CONH), 7.0-8.0 ppm (aromatic and olefinic protons in chalcone units), 6.2-6.5 ppm (N-CH-COO-), 5.3-5.6 ppm (OH), 3.85 ppm ($-\text{NCH}-$) and 0.8-2.3 ppm (CH_3 , CH_2 and CH).

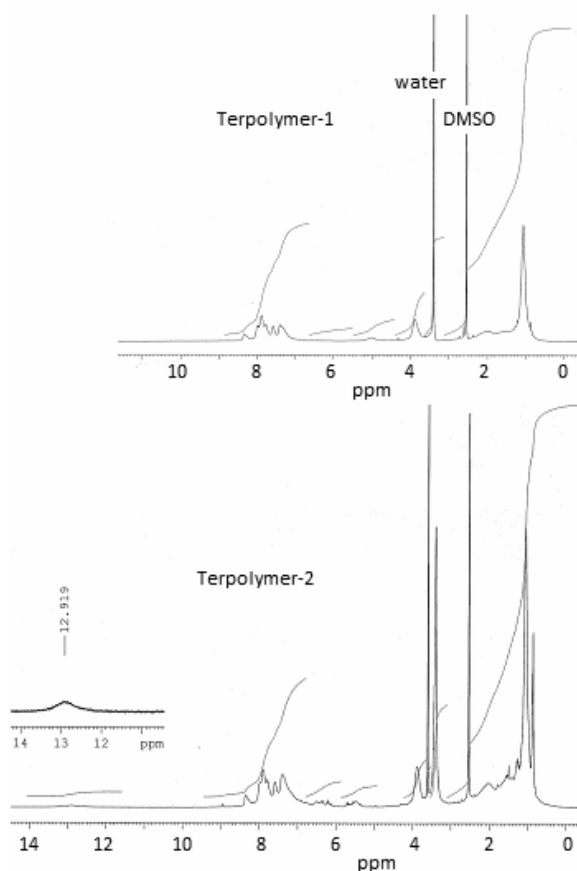


Fig. 2: ^1H -NMR spectra of terpolymer-1 and terpolymer-2.

Fluorescent spectra of terpolymer-1 and composite-1 were taken from the film samples. For an excitation wavelength of 529 nm the film shows a resonance emission at 525 nm for terpolymer-1. The composite-1 exhibits a double emission wavelength at 325 nm and at 680 nm for an excitation wavelength of 530 nm. This emission shift in the composite-1 can be caused by changing the number of emission sites on the surface of carbon nanotube

because of the oxidative treatment during the functionalization [21]

Photo-Crosslinking Studies of Polymers

The photo-crosslinking study of terpolymer-1 was carried out upon illumination with 365 nm light, and monitored by UV-visible spectroscopy. The quartz cell containing polymer solution with the concentration of 4 mg polymer / 25 mL solvent (dimethyl formamid, DMF) was kept at a distance of 12 cm from the UV lamp for different irradiation time. Immediately after each irradiation time intervals, the absorbance change at 345 nm was monitored (Fig. 3). The decrease in absorption at 345 nm was evident, which is attributed to the formation of cyclobutane rings through $[2\pi + 2\pi]$ cycloaddition of $\text{C}=\text{C}$ double bond in the chalcone unit. The maximum absorbance at $\lambda = 345$ nm of the $\text{C}=\text{C}$ double conjugated to the carbonyl group decreases fast upon UV illumination. At that same time, an increase of absorption is exhibited at 270 nm and at 413 nm attributed to the photochemical product. These behaviors of chalcones exposed to UV light were reported in many studies [22-25].

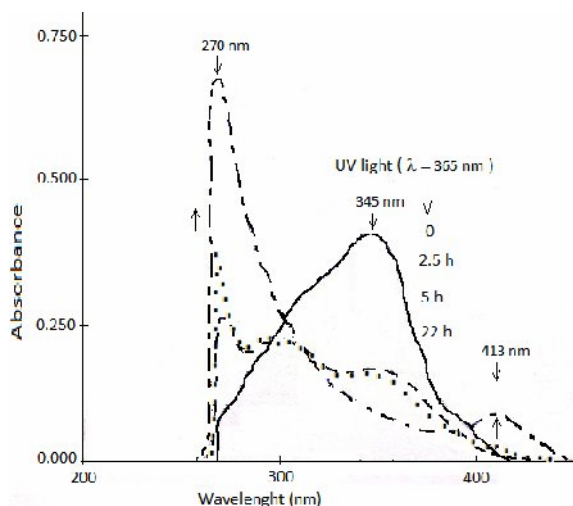


Fig. 3: UV-Visible spectral changes of terpolymer-1 upon UV irradiation.

The terpolymer-1 film prepared on salt plate was exposed to UV light for different irradiation time. After each irradiation time intervals, the FT-IR spectrum of the film was monitored (Fig. 4). Depending on the time of irradiation, intensities of ester carbonyl band at 1755 cm^{-1} and the carbon-carbon double bond band at 1612 cm^{-1} in units with chalcone were significantly reduced. These reductions indicate the changes in the chalcone units with UV irradiation.

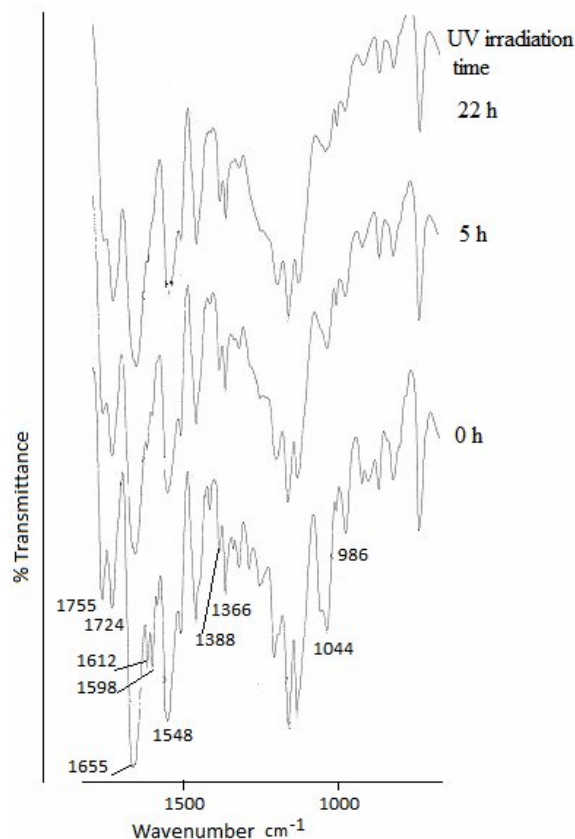


Fig. 4: FT-IR spectral changes of terpolymer-1 upon UV irradiation.

Thermal Characterization

A differential scanning calorimetry (DSC) curve (Fig. 5) for terpolymer-1 was generated using a DSC-50. The glass transition temperature of terpolymer-1 (as about 75 °C) was determined by DSC. Fig. 5 also show changing of dielectric constant (ϵ') with temperature. Dielectric constant increased moderately up to 75 °C, very slow between 75-120 °C and very fast after 120 °C with temperature. Dielectric constant is not change noticeably with temperature for nonpolar polymers whereas dielectric constant increases with temperature for strong polar polymers. The increase of the dielectric constant with temperature is due to an increase total polarization arising from dipoles and trapped charge carriers [26]. An increase in growth rate of specific volume slowed down the increase of dielectric constant between 75-120 °C. After 120 °C increase in the dielectric constant is dominated by an increase in specific volume. The expansion increases with increasing of temperature. The specific volume increases with increasing of expansion. The dielectric constants of these polymers increase for this reasons.

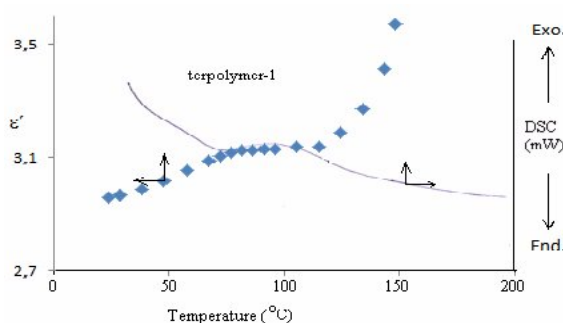


Fig. 5: The variation of dielectric constant(ϵ') and DSC trace with temperature of terpolymer-1.

The TGA curves for the MWNT-Ter-1, MWNT-Ter-2, terpolymer-1, composite-1 and composite-2 are shown in Fig. 6. Table-1 gives the thermal stability data of the polymers measured by TGA in nitrogen. Except a weight loss of about 2 % at 120 °C which is due to the expulsion of the moisture present in terpolymer-1, composite-1 and composite-2 the decomposition of all the polymers begin at about 300 °C. The MWNT-Ter-1 and MWNT-Ter-2 undergo two-stage decomposition. In the first step decomposition, they show a 30% weight loss in the temperature range of 295-455 °C, and then the MWNT-Ter-2 decomposes more rapid than the MWNT-Ter-1 in the second stage decomposition, which show a 12% residue and a 25% residue, respectively, at the end of the temperature range of 455-600 °C. The terpolymer-1 and nanocomposites (composite-1 and composite-2) undergo three-step thermal degradation processes. The first step degradation in the temperature range of 300-460 °C show a weight loss 55% for composite-1, 60% for composite-2 and 62%. In the second stage decompositions, a weight loss 10% in the temperature range of 460-550 °C for the composite-1 and terpolymer-1 and a weight loss 10% in the temperature range of 460-520 °C for the composite-2 occur. Having a weight loss 10% in this temperature range of these polymers implies that their thermally stable probable due to formation of cyclic imide structures with a reaction between adjacent N-isopropylacrylamide units by heating up to 460 °C [27] all the polymers left a constant residue lower than 10% at about 650 °C. From these Figs the high thermal stability of the MWNT-Ter-1, MWNT-Ter-2 and low thermal stability of the terpolymer-1 and the nanocomposites can be seen. The thermal stabilities of the MWNT-Ter-1 and MWNT-Ter-2 are lower than that of MWNT which its decomposition starts at about 500 °C (no TGA curve) due to activation its surface of free radicals generated during decomposition of polymer on the surface of the MWNT [28].

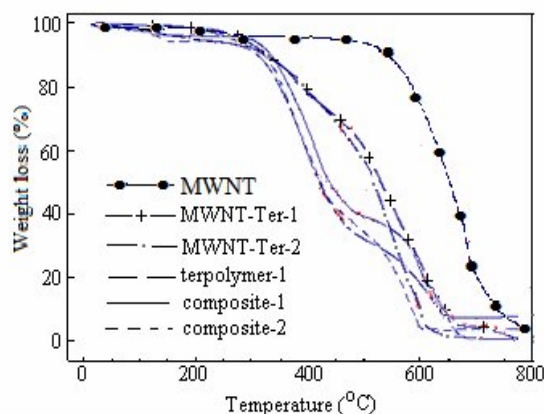


Fig. 6: TGA curves of the substances studied.

Dielectrical and Electrical Properties

The general trend of conductivity is to increase according to increase in frequency. Fig. 7 shows real part of the permittivity (ϵ') and the ac conductivity as function of frequency for the composites and the polymers. The composite-1 shows ac conductivity higher than that of the terpolymer-1, and the ac conductivity of composite-1 increases largely in comparison to terpolymer-1 and thus the difference between their conductivities increases with increasing frequency. According to Fig. 7, while the values of ϵ' of terpolymer-1 and composite-1 decrease a little faster up to about 3 kHz, and then remains nearly constant with increasing frequency, but the values of ϵ' of composite-2 constant. As be seen in Fig. 7, the conductivity of composite-1 increases with rise temperature. Such a character of the temperature dependence can be attributed both to ionic and electronic type of conductivity [29]. Thus, the both electrons and ions contribute to the conductivity of composite-1.

In this study, we synthesized and characterized the novel polymer coated MWCNT/Terpolymer composites. Such composites can be used as photo-sensitive materials. We hope that this original work is potentially a useful addition to the literature and can guide to some high polymer works.

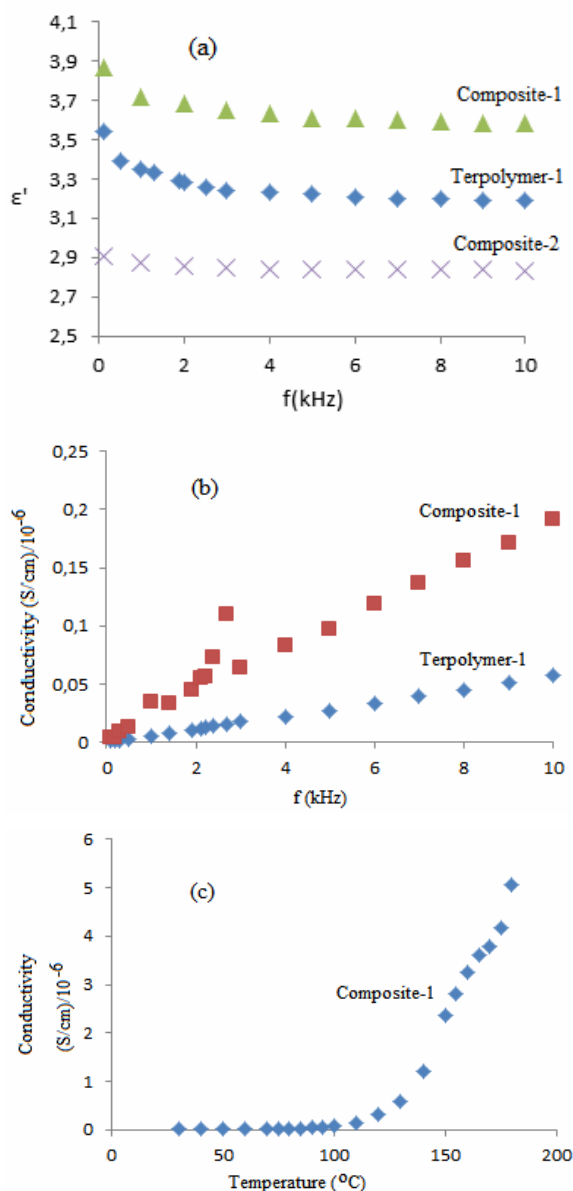


Fig. 7: Variation of dielectric constant with frequency for terpolymer-1, composite-1 and composite-2 (a), and conductivity with frequency for terpolymer-1 and composite-1(b), and conductivity with temperature for composite-1 (c).

Table-1: TGA data for the polymers.

polymers	T ₁ ^a [°C]	Stage 1 Temperature Range	Weight Loss in Stage 1 (%)	Stage 2 Temperature Range	Weight Loss in Stage 2 (%)	Stage 3 Temperature Range	Weight Loss in Stage 3 (%)	Residue (%)
MWNT-Ter-1	295	295-455	30	455-600	45			25
MWNT-Ter-2	295	295-455	30	455-600	58			12
Terpolymer-1	300	300-460	62	460-550	10	550-605	20	8
Composite-1	300	300-460	55	460-550	10	550-650	26	9
Composite-2	300	300-460	60	460-520	10	550-605	22	8

^a Initial decomposition temperature.

Conclusions

In preparation of composites, the first MWNT have been coated by covalently bonding with terpolymer, and then the MWNT coated the polymer has been dispersed in terpolymer solution. The powder composite was prepared by together precipitation of the coated MWNT and the terpolymer from the solution. Terpolymers and composites were characterized structurally by ^1H -NMR and FT-IR spectra. For an excitation wavelength of 529 nm the film shows an emission at 525 nm for terpolymer-1, but the composite-1 exhibit a double emission wavelength at 325 nm and at 680 nm for an excitation wavelength of 530 nm.

The chalcone units in terpolymer used to prepare the composite exhibited photo-crosslinking behavior when expose to UV irradiation.

Thermal stabilities of terpolymer-1, MWNT-Ter-1, MWNT-Ter-2, composite-1 and composite-2 are very lower than that of the MWNT because of the organic groups attached to the others except MWNT

The composite-1 shows ac conductivity higher than that of the terpolymer-1, and the ac conductivity of composite-1 increases largely in comparison to terpolymer-1 and thus the difference between their conductivities increases with increasing frequency.

References

1. Z. Spitalsky, D. Tasis, K. Papagelis and C. Galiotis, Carbon nanotube-polymer Composites: Chemistry, processing, mechanical and electrical properties, *Prog. Polym. Sci.* **35**, 357 (2010).
2. W. D. Wang, P. Serp, P. Kalck and J. L. Faria, Visible light photodegradation of phenol on MWNT-TiO₂ composite catalysts prepared by a modified sol-gel method, *J. Mol. Catal. A: Chem.*, **235**, 194 (2005).
3. G. Lota, K. Lota and E. Frackowiak, Nanotubes based composites rich in nitrogen for supercapacitor application, *Electrochem. Commun.*, **9**, 1828 (2007).
4. P. M. Ajayan and S. Iijima, Capillarity-induced filling of carbon nanotubes, *Nat.*, **361**, 333 (1993).
5. A. Bachtold, P. Hadley, T. Nakanishi and C. Dekker, Logic circuits with carbon nanotube transistors, *Sci.*, **294**, 1317 (2001).
6. P. V. J. Kamat, Meeting the clean energy demand: Nanostructure architectures for solar energy conversion, *Phys. Chem.*, **111**, 2834 (2007).
7. Y. Chen, C. Zhu and T. Wang, The enhanced ethanol sensing properties of multi walled carbon nanotubes/SnO₂ core Shell nanostructures, *Nanotech.*, **17**, 3012 (2006).
8. H. C. Huang, G. L. Huang, H. L. Chen and Y. D. Lee, Immobilization of TiO₂ nanoparticles on carbon nanocapsules for photovoltaic applications, *Thin Solid Films*, **511**, 203 (2006).
9. X. L. Xie, Y. W. Mai, X. P. Zhou, Dispersion and alignment of carbon nanotubes in polymer matrix: A review, *Mater. Sci. Eng.*, **R 49**, 89 (2005).
10. N. G. Sahoo, S. Rana, J. W. Cho, L. Li and S. H. Chan, Polymer nanocomposites based on functionalized carbon nanotubes, *Prog. Polym. Sci.*, **35**, 837 (2010).
11. J. H. Du, J. B. H. M and Cheng, The present status and key problems of carbon nanotubes based polymer composites, *Express Polymer Letters*, **1**, 253 (2007).
12. Y. Lin, A. M. Rao, B. Sadanadan, E. A. Kenik and Y. Sun, Functionalizing Multiple-Walled carbon nanotubes with aminopolymers, *Journal Physical Chemistry B*, **106**, 1294 (2002).
13. B. Pan, D. Cui, R. He, F. Gao and Y. Zhang, Covalent attachment of quantum dot on carbon nanotubes, *Chem. Phys. Lett.*, **417**, 419 (2006).
14. H. T. Ham, C. M. Koo, S. O. Kim, Y. S. Choi and I. J. Chung, Chemical modification of carbon nanotubes and preparation of polystyrene/carbon nanotubes composites, *Macromolecular Research*, **12**, 384 (2004).
15. P. M. Ajayan, O. Stephan, C. Colliex and D. Trauth, Aligned carbon nanotube arrays formed by cutting a polymer resin-nanotubes composite, *Sci.*, **265**, 1212 (1994).
16. L. Chen, X. J. Pang, M. Z. Qu, Q. T. Zhang, B. Wang, B. L. Zhang and Z. L. Yu, Fabrication and characterization of polycarbonate/carbon nanotube composites, *Compos. Part A* **37**, 1485 (2005).
17. R. Andrews and M. C. Weisenberger, Carbon nanotubes polymer composites, *Curr. Opin. Solid State Mater. Sci.*, **8**, 31 (2004).
18. A. Kanapitsas, C. Tsonos, D. Triantis, E. Logakis, C. Pandis, P. Pissis, Proceedings of the 1st WSEAS International Conference on Nanotechnology (Nanotechnology'09) p 75-81, (2009).
19. A. Chiolerio, M. Castellino, P. Jagdale, M. Giorcelli, S. Bianco and A. Tagliaferro Carbon Nanotubes Polymer Nanocomposites Edited by Dr. Siva Yellampalli, Published online 17 August, **215** (2011).

20. D. Coşkun and M. Ahmedzade, 3-(Substituted Aryl)1-(Benzofuran-2-yl)-2-Propenones, Part:1 Synthesis and Characterization of Some Novel Chalcones, *Synth. Commun.*, **38**, 3613 (2008).
21. L. Minati, G. Speranza, I. Bernagozzi, S. Torrenço, A. Chiasera, M. Ferrari and D. Related, Luminescent short thiol functionalized multi-wall carbon nanotubes, *Mater.*, **20**, 1046 (2011).
22. S. H. Kim, C. H. Ahn, S. R. Keum and K. Koh, Synthesis and properties of spiroxazine polymer having photocrosslinkable chalcone moiety, *Dyes Pigments*, **65**, 179 (2005).
23. H. Wünscher, G. Haucke and P. Czerney, Photochromic properties of hydrolysed benzopyrylium salts-the influence of bridging, *J. Photochem. Photobiol.*, **152**, 61 (2002).
24. D. H. Choi and S. J. Oh, Photochemical reactions of a dimethacrylate compound containing a chalcone moiety in the main chain, *Eur. Polym. J.*, **38**, 1559 (2002).
25. M. Guo and X. Wang, Polyimides with main-chain photosensitive groups: Synthesis, characterization and their properties as liquidcrystal alignment layers, *Eur. Polym. J.*, **45**, 888 (2009).
26. V. Rao, P.V. Ahokan, M.H. Shridhar, Studies of dielectric relaxation and a.c. conductivity in cellulose acetate hydrogen phthalate-poly(methyl methacrylate) blends, *Mater. Sci. Eng. R*, **A281**, 213 (2000).
27. M. Coskun, M. M. Temuz and K. Demirelli, Characterization and thermal degradation of poly(2-methacrylamidopyridine), *Polym. Degrad. Stab.*, **77**, 371 (2002).
28. S. P. Shaffer and A. H. Windle, Fabrication and Characterization of Carbon Nanotube/Poly(vinyl alcohol) Composites, *Adv. Mater.*, **11**, 937 (1999).
29. Y. P. Mamunya, V. V. Levchenko, A. Rybak, G. Boiteux, E.V. Lebedev, J. Ulanski and G. Seytre, Electrical and thermomechanical properties of segregated nanocomposites based on PVC and multiwalled carbon nanotubes, *J. Non-Cryst. Solids*, **356**, 635 (2010).